JPPIPA 8(3) (2022)

Jurnal Penelitian Pendidikan IPA

Journal of Research in Science Education

http://jppipa.unram.ac.id/index.php/jppipa/index

Observation of Rayleigh Benard Convection as A Representation of Learning of Natural Phenomenons Through Water Molecular Movement

M. Hidayatur Rohman[1,2], Putut Marwoto[3], Retno Sri Iswari[3], Edy Cahyono[3]

[1] Student of Doctoral Science Education Postgraduate Program, Universitas Negeri Semarang, Semarang, Indonesia
[2] Physics Education Study Program, IAIN Salatiga, Salatiga, Indonesia
[3] Science Education Postgraduate Program, Universitas Negeri Semarang, Semarang, Indonesia.

DOI: 10.29303/jppipa.v8i3.1323

Article Info
Received: January 13, 2022
Revised: June 15, 2022
Accepted: July 20, 2022
Published: July 31, 2022

Abstract: Research has been carried out with a device to observe the phenomenon of Rayleigh Benard convection, made of a glass box bounded by a lower plate and an upper plate. The bottom plate is hotter than the top plate which functions to heat the horizontal fluid layer from below. This study aims to observe the phenomenon of water molecule movement. The observation medium was water mixed with teak sawdust as a representation of water particles with an average density of mean=0.99 g/cm^3. The variation of water thickness (d) used 5 cm and 6 cm with variations in temperature difference (ΔT) with an average increase of 50°C. Data was collected with a cellphone camera and run with Windows Movie Maker software which has a time accuracy of up to 0.001 seconds. It was observed that an increase in the temperature difference (ΔT) between the two plates resulted in an increase in the velocity of motion of water particles in convection which is depicted by a v-ΔT diagram. Due to the difference in temperature (ΔT) also results in the movement patterns of water molecules, namely laminar and turbulent. The turbulent phase with the Rayleigh number value R~10^7, indicated that the flow of water particles is getting faster, the direction of the flow of the particles starts to become irregular and sometimes signs of a water vortex appear. At different fluid immersion results in the start of a turbulent phase. The turbulent phase for d=5cm is observed at ΔT~30°C, and d=6cm at ΔT~20°C. Furthermore, this RBC phenomenon is used as a representation of learning natural phenomena in air fluids, namely whirlwinds as an event due to differences in temperature and pressure of a fluid.

Keywords: Rayleigh Benard convection; Laminar and turbulent; Bifurcation diagrams; Whirlpools; Whirlwinds.

Citation: Rohman, M. H., Marwoto, P., Iswari, R.S., & Cahyono, E. (2022). Observation of Rayleigh Benard Convection as A Representation of Learning of Natural Phenomenons Through Water Molecular Movement. *Jurnal Penelitian Pendidikan IPA*, *8*(3), 1074–1082. https://doi.org/10.29303/jppipa.v8i3.1323

Introduction

The convection phenomenon is an example of the heat instability problem in the fluid layer caused by temperature differences. For convection that occurs in the horizontal layer of fluid, it is known as Rayleigh Benard Convection (RBC) (Getling, 1997). RBC is an important phenomenon to determine fluid dynamics caused by heating from below (Getling, 1997), the flow occurs between two parallel plates with different temperatures, namely when the temperature of the lower plate is higher than the upper plate (Ayed, S.K. & Tomic, 2017). The main concern of RBC is to study the instability in the fluid caused by thermal expansion, so that there is an increase and decrease in fluid temperature (the lower fluid is hotter than the upper fluid) (Ayed, S.K. & Tomic, 2017). The phenomenon of convection of a fluid is influenced by its properties, namely viscosity, density, thermal expansion, and heat diffusion or thermal

* Corresponding Author: hidayat80@students.unnes.ac.id

conductivity. The convection heat transfer coefficient is strongly influenced by flow hydrodynamics. Changes in flow patterns and velocity will affect the ability of the fluid to transfer heat (energy) (Sudia, 2017). Convection is also determined by the thickness of the fluid (d) and the temperature difference between the two plates (δT) (Ayed, S.K. & Tomic, 2017).

Many later theoretical and experimental studies of RBC were carried out by scientists. The theoretical study of RBC using the numerical method was carried out using multi-scale analysis and asymptotic expansion method (Fan, et. al., 2020) the 2D pseudo-spectral method in the MATLAB code for the Navier-Stokes equation (Ayed, et. al., 2016), a pseudo-spectral method based on Fourier (Ramos and Briozzo, 2015), the Lattice Boltzmann Simulation method (Nataraj, et. al., 2017); Cai, et al. 2018; Yang & Liu, 2018), and nonlinear analysis based on the power-series method to obtain eigenvalues (Siddheshwar and Krishna, 2001). Green, et. al., (2020) investigated RBC using direct numerical simulations (DNS) in a large aspect ratio system from a weak nonlinear regime close to the onset to a turbulent regime covering the Rayleigh number range from $Ra=10^4$ to $Ra=10^8$ at Pr = 1, whereas (Palymskiy, 2015) with DNS on the Boussinesq approach without a semiempirical relationship.(Zhou, et. al., 2019) calculated the RBC flow using the Maxwell numerical integration method under the Rytov approach. (Pandey, et. al. 2018) also used numerical simulations of the turbulent convection fluid RBC at different Prandt numbers ranging from 0.005 to 70 and for the Rayleigh numbers to 10^7, previously the kinetic energy spectrum Eu (k) for three-dimensional convective turbulence in the RBC system was also observed numerically by (Bhattacharjee, 2015). (Lyubimova, et. al., 2015) studied the Marangoni effect at the onset of RBC numerically in the framework of the generalized Boussinesq approach using the Busse-Lyubimov model. The numerical procedure was also performed by (Chen, et. al., 2015) based on the Navier-Stokes equation coupled with the energy equation and nonlinear properties of CO_2 to observe the nearly critical Poiseuille Rayleigh-Benard CO_2 convective flow in the micro channel.

Scientists are also researching RBC experimentally, including (Aurnou, J.M. & Olson, 2001) examined the experimental thermal convection in a liquid gallium layer subject to uniform rotation and a uniform vertical magnetic field carried out as a function of rotation rate and magnetic field strength. (Balasubramanian, S. & Ecke, 2013) studied the heat transport mechanism in RBC which rotates along the vertical axis. (Ayed, S.K. & Tomic, 2017) conducted an RBC experiment on natural convection depending on the geometric relationship and surface temperature, and determined the type of flow, whether laminar or turbulent. RBC experiments were also carried out by making RBC observation devices ((Rohman, 2019); (Suparso, et. al., 2010)). This RBC observation device is made of a glass box bounded by two plates, namely the lower plate and the upper plate. The lower plate is hotter than the upper plate which serves to heat the horizontal layer of fluid from below. The media used to observe fluid dynamics is water mixed with teak sawdust (SGKJ) as a representation of water particles. Furthermore, RBC observations were also carried out on oil fluid (Yustin, R. & Yusuf, 2013).

The first scientists to explain RBC experimentally and theoretically were Henri Benard in 1900 and Lord Rayleigh in 1916. Both scientists produced Benard cells which are symptoms of convection in fluid (water) observed from above (Figure 1), and the parameters are numberless. Rayleigh (equation 1) ((Ahlers, 2006); (Balasubramanian, S. & Ecke, 2013); (Ayed, S.K. & Tomic, 2017); (Klein, et. al., 2018); (Klein, M. & Schmidt, 2019)),

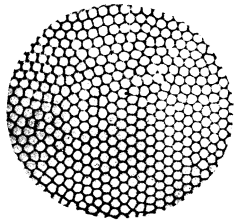

Figure 1. *Benard cell* (Ayed & Tomic, 2017)

$$R = \frac{\alpha g d^3 \Delta T}{\kappa \nu} \quad (1)$$

where α is the coefficient of thermal expansion, κ the coefficient of thermal diffusion, ν the coefficient of kinematic viscosity, d the distance between two plates, g of gravitational acceleration, ΔT of temperature difference and R is known as the Rayleigh number (Rayleigh Number). Rayleigh also explained that convection occurs when the Rayleigh number (R) is greater than the critical Rayleigh number (Rc), with Rc = 1708 (Ayed, et. al. 2016), or has the order 10^3 (Aurnou, J.M. & Olson, 2001).

The type of flow of particles of a fluid can be viewed from the Rayleigh number (R) value, namely For R <Rc, there is no particle flow or convection has not occurred (Ayed, et. al., 2017). For R> Rc, but not very large, a regular structure of convection circles forms (Figure 2) with upward hot fluid and downward cold fluid (Ayed, et. al., 2017). Convection flow of particles is a type of laminar flow and For R >> Rc, there is a turbulent flow, namely $R \geq 4 \times 10^7$ (Jiji, 2006). Broadly speaking, the flow of fluid particles is divided into two, namely laminar and turbulent (Jiji, 2006). However, there is a phase between laminar and turbulent which is often called the transitional phase. The Rayleigh number (R) for the phase transition ranges from 10^5 to 10^6. In the turbulent phase there is also a transition phase between weak and strong turbulence, the value ranges between $R=10^7$ and 4×10^7 (Hui Peng, et. al., 2006). RBC is an

important phenomenon to determine fluid dynamics caused by heating from below (Getling, 1997), the flow occurs between two parallel plates with different temperatures, namely when the temperature of the bottom plate is higher than the upper plate (Ayed, et. al., 2017)

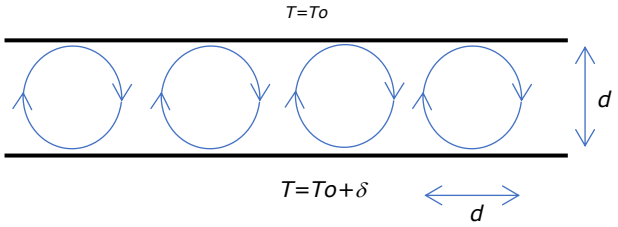

Figure 2. Convection scheme (Ayed, et. al., 2017)

RBC is considered by many scientists to play a role in research on natural phenomena. As was done by (Grigoriev, V.V. & Zakharov, 2017) states that convection in a horizontal liquid layer that is heated from below and cooled from above, or RBC is the type of convection most often considered. RBC plays an important role in various phenomena in the fields of geophysics, astrophysics, meteorology, oceanography and engineering. Turbulent superstructures in RBC, namely large-scale flow structures in turbulent flow, play an important role in many geo and astrophysical arrangements ((Pandey, et. al., 2018; Green, et. al., 2020). RBC's natural convection heat transfer occurs on a variety of smaller scales (in pipelines, canals, and tanks) to large scales (atmosphere, liquid planet essence) which have been studied for a long time for their energy benefit (Ayed, et. al., 2017).

Several scientists found the type of fluid flow in their research on RBC, namely laminar and turbulent flow (Jiji, 2006). However, there is a phase between laminar and turbulent which is often called the transitional phase. The transition phase between laminar and turbulent at R values between 10^6 to 10^7 (Gayen, et. al., 2014; Berdnikov, et. al., 2018). The thing that attracts the attention of scientists in research on RBC related to natural phenomena is the turbulent phase. The turbulent phase occurs when R >> Rc, that is, with a value of $R \geq 4\times10^7$ ((Ahlers, et. al., 2017); Klein, et. al., 2018). Pandey, et. al. (2018) and Green, et. al., (2020) observed the turbulent superstructure at Rayleigh numbers up to 10^7, Stevens, et al. (2018) to Rayleigh $Ra=10^9$, Rayleigh number $Ra=\sim2\times10^9$ (Palymskiy, 2015). (Valencia, et. al., 2007) observed natural convection in cube cavities heated from below and cooled from above at Rayleigh turbulent numbers $Ra=10^7$, $Ra=7x10^7$ and $Ra=10^8$, while (Balasubramanian, S. & Ecke, 2013) observed Rayleigh-Bénard turbulent convection in a rotating frame. and non-rotating in square cross section at Rayleigh number, $R=1x10^7$-$2x10^8$. The laminar phase is marked by the phenomenon of convection and not so fast motion of water particles. Turbulent flow is characterized by an irregular flow of water particles (chaos). A chaotic state can be observed by observing the motion of particles that change suddenly, dramatically and tend to fluctuate, which is marked by the appearance of whirlpool symptoms with unpredictable frequency of appearance (Rohman, 2019). This whirlpool symptom can then be used as a representation of science learning about natural phenomena that occur in fluids (water/air).

The research was carried out using the RBC observation device as described above with the bottom plate as a heater made of a glass box filled with water heated with a heating element. The top plate is also made of a glass case filled with water at room temperature. The increase in the temperature difference between the two plates results in an increase in the velocity of the motion of water particles during convection which is depicted by a v-ΔT diagram ((Suparso, et. al., 2010); (Yustin, R. & Yusuf, 2013)). The increase in ΔT also results in changes in the movement patterns of water particles (laminar and turbulent). In this study, laminar and turbulent patterns were observed due to the greater ΔT. So that complete information will be conveyed for each phase with an image of the water particle movement pattern represented by SGKJ. The whirlpool phenomenon can then be used as a learning representation of the occurrence of the natural phenomenon of whirlwinds in science lessons. To simplify the problem, several limitations are used in this study. These limitations include, the fluid used is water mixed with SGKJ, the calculation of the velocity of the water particles uses the mean velocity and is shown in the v-ΔT diagram, while the flow pattern of water particles for each phase will be displayed by describing the direction of motion of the water particles at each increasing difference. temperature (ΔT). Furthermore, this water fluid is used as a representation of air/wind fluid.

As the purpose of this study is to observe the RBC convection menomena which will be used as a representation to explain natural phenomena, then the definition of examples of natural phenomena about whirlwinds will be described. Whirlwinds are defined as strong winds that come suddenly, have a center, move in a circle resembling a spiral at a speed of 40-50 km / hour to touch the earth's surface and will disappear in a short time (3-5 minutes) (Utomo, 2016) , or strong winds that spin out of the Cumulonimbus cloud with a speed of more than 34.8 Knots or 64.4 km/h and occur in a short time (Marselina, D.S. & Widodo, 2015). Whirlwinds are caused by differences in pressure in a weather system due to differences in air temperature. This pressure difference produces a pressure gradient that triggers the wind. Air moves from high pressure to low pressure and the higher the pressure difference, the faster the air moves (Handoko, 1995). The process of whirlwinds usually occurs during the transition season where during the daytime the temperature of hot, stuffy air and black clouds collect, as a result of solar radiation during the day, clouds form vertically (convective) with a lowpressure center, then in the cloud it occurs

turbulence or instability of air currents rising and falling at a fairly high speed. Air currents that fall at high speed blow to the earth's surface suddenly and travel randomly (Utomo, 2016). The occurrence of a tornado goes through three phases, namely; Growing phase, in the cloud there is a strong upward air current. The rain has not yet fallen, the water droplets and ice crystals are still being held back by the air currents that rise above the cloud tops. Adult / mature phase, water droplets are no longer held back by the air rising to the top of the cloud. The falling rain creates a friction force between the rising and falling air currents. The temperature of this falling air mass is colder than the surrounding air. Between the rising and falling air currents there can be shear currents that twist, forming a vortex. This air current is spinning faster and faster, like a cyclone "licking" the earth as a tornado. This wind is sometimes accompanied by heavy rain which forms a water spout (Utomo, 2016). By comparing the similarity in the process of whirlpools that appear in this study with the process of whirlwind, it is expected that this study is representative.

Method

This RBC phenomenon research is carried out in several stages, including designing (Figure 3), testing, and setting up observation devices (Figure 4). After the tool is confirmed to show the convection phenomenon, the next step is to observe the RBC phenomenon. In detail, this observation can be explained by observing Figure 3 and Figure 4. The initial steps taken can be explained in Figure 3. First, take water at room temperature and fill it in sections 1, 2, and 3. Part 2 water is mixed with SGKJ which has known the average density ($\rho_{average}$=0.99 g/cm^3) and let the water return to a calm state. Second, ensuring the water temperature is the same (at room temperature) in sections 1 and 3 with the thermometer, then the thermometer is used to control the temperature difference during the observation.

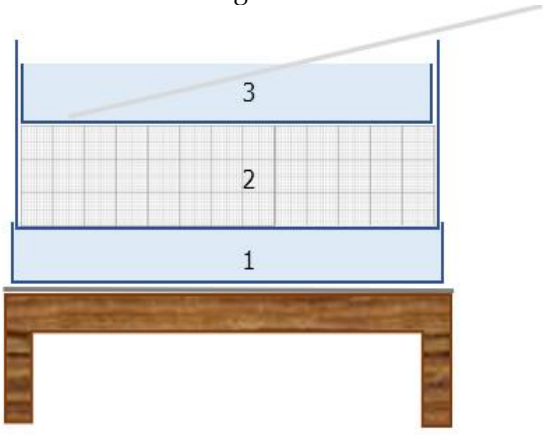

Figure 3. Schematic of the observation instrument

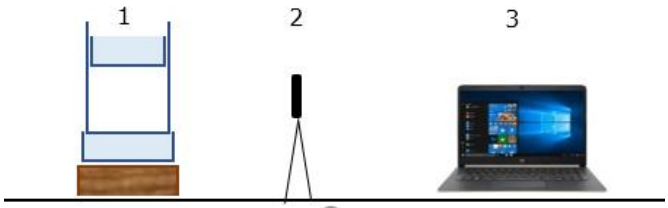

Figure 4. Schematic of the RBC observation device set-up

Third, connect the plug to the electric current to heat the heating element, so that the water temperature of part 1 is hotter than part 3 and the temperature difference between the bottom plate and the top plate will be obtained. The difference in temperature can be seen by looking at the numbers that appear on the thermometer installed in sections 1 and 3. Then to set the desired temperature, part 1 is adjusted using a switch, while section 3 is stabilized at room temperature using ice. Fourth, make observations on changes in water fluid dynamics in section 2 for some temperature differences, then these changes are recorded with a cellphone camera (Figure 4). At the time of recording, the temperature difference is confirmed to be stable, namely by cutting the current flowing in the strika element and recording for 1.5 minutes. This is done because considering the nature of water that can conduct heat evenly and is relatively long in maintaining its temperature. Fifth, observing the results of the recording using a laptop (Figure 4), then taking and analyzing the data obtained from the recording results. The data taken is the velocity of the motion of water particles as a function of temperature differences, so that the movement can be known about the grouping of flow patterns of laminar or turbulent water particles. Laminar and turbulent patterns were also observed for variations in fluid thickness.

The data was collected by running Windows Movie Maker software which has a time accuracy of up to 0.001 seconds. After the Windows Movie Maker software is run, data is taken for the speed and flow pattern of water particles, how to mark the dots on the computer screen using a marker when the Windows Movie Maker is stopped by pressing the pause button. Data obtained from observations can be in the form of qualitative and quantitative data, so that the analysis will have different techniques. For qualitative data, the analysis is carried out by interpreting the data obtained, while for quantitative data it is analyzed based on formulas that are in accordance with the needs. For velocity data, the steps taken are to record the displacement distance and the time interval, then divide the displacement distance by the time interval. In order to obtain a representative average velocity, each particle is calculated three times at different positions. Furthermore, the flow pattern of water particles can be observed by interpreting the resulting lines connecting the dots on a computer screen, such as a step made in a velocity observation. Laminated flow is a regular flow pattern, characterized by a convection flow pattern. Points connected to form a circular part (semicircle or

circle), or ellipse, or which appear to be a straight vertical line, are signs of a convection flow pattern. For turbulent flow patterns characterized by irregular circles, and very fast particle movements.

Result and Discussion

This study uses a tool for observing the Rayleigh Benard convection phenomenon as shown in Figure 5, in the form of a box made of glass with water mixed with SGKJ as the observation medium. The mean density was measured by an automatic densimeter, with the result $\rho_{average}$=0.99 g/cm^3, and observed using a cellphone camera. The results of the recordings were then analyzed by computer as shown in Figure 6. After there is a difference in temperature, water particles begin to move which are represented by the SGKJ movement as shown in Figure 7.

Figure 5. Photo of the RBC observation instrument

As mentioned above, the main concern of RBC is studying the instability in the fluid caused by thermal expansion, so that there is an increase and decrease in fluid temperature (the lower fluid is hotter than the upper fluid) (Ayed, S.K., Zivkovic, P. & Tomic, 2017).

Figure 6. Photo of RBC observation device set up

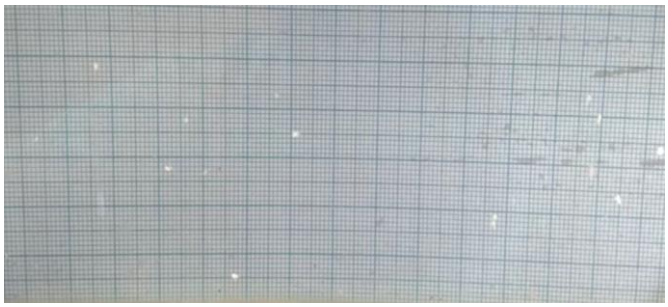

Figure 7. Snapshot of one of the RBC observations

Figure 7 shows the observations that have been made of the RBC phenomenon using the RBC observation instrument, information is obtained about the effect of increasing temperature differences between the upper and lower plates on the velocity of motion of water particles and the flow patterns of water particles. At the time of observing the flow pattern of water particles, it was observed that the vortex phenomenon of water particles appeared. As it is known that the type of particle flow of a fluid can be viewed from the Rayleigh number (R) value, namely for R<Rc, there is no particle flow or convection has not occurred (Ayed, et. al., 2017). For R>Rc, but not very large, a regular structure of convection circles forms (Figure 1) with upward hot fluid and downward cold fluid (Ayed, S.K., Zivkovic, P. & Tomic, 2017). Convection flow of particles is a type of laminar flow (Jiji, 2006), and for R>>Rc, there is a turbulent flow, namely R=4x10^7 (Ayed, et. al., 2017; Klein, et. al., 2018). RBC observations in this study used variations in T with an average increase of 5oC, while the thickness of the water used was 5 cm and as a comparison, the water thickness was 6 cm.

Observation of the speed of motion of water particles

Observation of the velocity of water particles obtained a graph of the relationship between v and T which is a v-ΔT diagram (Figure 8 and Figure 9). The increase in the temperature difference between the two plates results in an increase in the velocity of the water particles at convection which is represented by a v-ΔT diagram. Figure 8 is a v-ΔT diagram, with the velocity of water particles (v) clockwise and Figure 9 shows a v-ΔT diagram, with the velocity of water particles (v) counterclockwise.

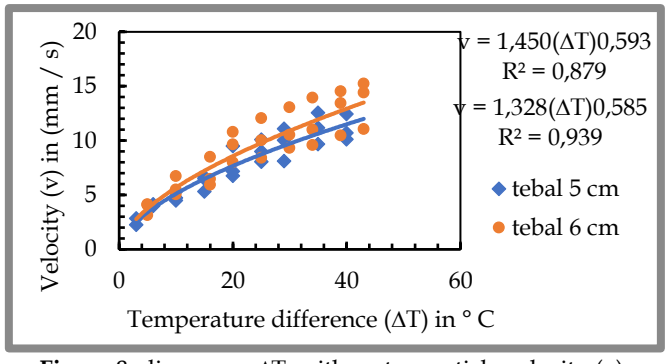

Figure 8. diagram v-ΔT, with water particle velocity (v) clockwise for water thickness of 5 cm and 6 cm

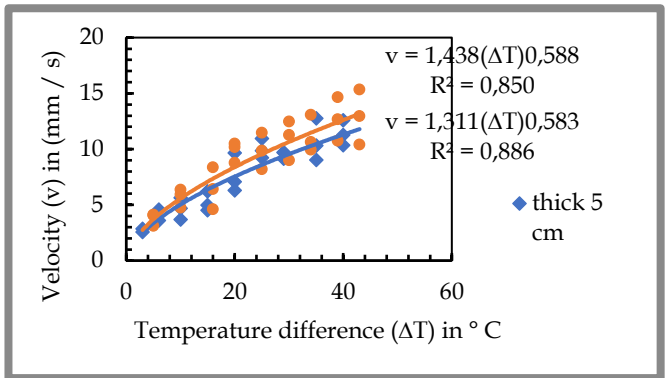

Figure 9. diagram v-ΔT, with particle velocity (v) counterclockwise for a water thickness of 5 cm and 6 cm

Based on Figure 8 and Figure 9, it can be seen that the speed of motion of water particles has increased due to the increase in temperature differences. Fitting to the graph above Figure 8 shows that the increase in the velocity of the motion of the water particles follows an equation $v_{(d=5)} \sim 1{,}4(\Delta T)^{0{,}59}$ and $v_{(d=6)} \sim 1{,}3(\Delta T)^{0{,}58}$ and figure 9 follow the equation $v_{(d=5)} \sim 1{,}4(\Delta T)^{0{,}58}$ and $v_{(d=6)} \sim 1{,}3(\Delta T)^{0{,}58}$. These results can be compared with the branching diagram theory which shows that the increase in velocity corresponds to the equation $v \sim R^{0,5}$ ((Drazin, 2002). From equation 1 it is known that the number R is proportional to the value of ΔT. Therefore, a branching diagram theoretical approach can be applied to the increase of v by ΔT with an equation $v \sim (\Delta T)^{0,5}$. The results of the graph fittings show that for water thickness of 5 cm and 6 cm, each of them has almost the same suitability for the increase in velocity, namely $v \sim (\Delta T)^{0,6}$. The comparisons made show that the observations are close to the theory.

Table 1. Physical properties of water (Welty, et. al., 2001)

T (°C)	ρ (g/cm³)	$c_v \times 10^{-7}$ (ergs/g °C)	$\kappa \times 10^4$ (cm²/s)	ν (cm²/s)	$\alpha \times 10^3$ (°C)$^{-1}$
20	0.998	4.19	14.33	$1{,}006 \times 10^{-2}$	2.0
40	0.992	4.18	15.11	$6{,}58 \times 10^{-3}$	3.8

Interpretation of the difference in critical temperature (ΔT_c) can also be done using the v-ΔT diagram in Figure 8 and Figure 9. By using the equations in the graph and the approximate value of v = 0.05 mm / s, it can be seen that the value of ΔT_c for water thickness 5 cm and 6 cm, are 0.00363 ° C and 0.00353 ° C, respectively. The results of the interpretation can be compared with the results of calculations using equation 1 which is a dimensionless parameter of the Rayleigh number ((Ahlers, 2006); (Balasubramanian, S. & Ecke, 2013); (Ayed, S.K. & Tomic, 2017); (Klein, et. al., 2018); (Klein, M. & Schmidt, 2019)). Rayleigh also explained that convection occurs when the Rayleigh number (R) is greater than the critical Rayleigh number (Rc), with Rc = 1708 (Ayed, et. al., 2016), or has the order 10^3 (Aurnou, J.M. & Olson, 2001). It is known that the critical Rayleigh number (Rc) for the occurrence of convection is 1708.Then an approach is made to the physical properties values as shown in Table 1. The physical values used are around 30°C or values between 20°C and 40°C, and obtained the value of κ=14,73×10⁴ cm²/s, ν=8,32×10³ cm²/s, and $\alpha = 2{,}9 \times 10^3$ (°C)$^{-1}$. From the calculation, it is known that the values of ΔT_c for the thickness of d = 5 cm and d = 6 cm are 0.00589°C and 0.00341°C. Thus, the observed ΔT_c value is close to the calculation result (theory).

Observation of the flow pattern of water particles

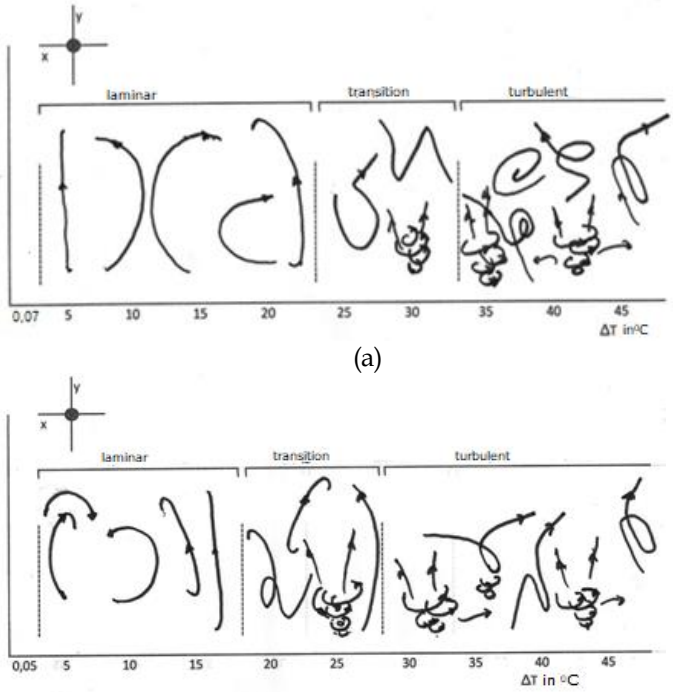

Figure 10. Schematic flow pattern of water particles, (a) flow pattern at water thickness of 5 cm, and (b) flow pattern at water thickness of 6 cm

Figure 10 shows a schematic flow pattern of water particles. Researchers showed that the flow patterns of water particles were deliberately drawn manually according to those observed on a computer screen. This is because it is difficult to make a water particle flow pattern animation program. The problem of heat instability in a fluid (water) caused by heating from below can also be observed by observing the flow pattern of the water particles. Heat instability in water will cause heat transfer which is followed by water particles forming a certain flow pattern. The flowing water particles follow two flow patterns, namely laminar and turbulent (Jiji, 2006). In this study, laminar flow is characterized by the phenomenon of convection and not so fast motion of water particles. Turbulent flow is characterized by an irregular flow of water particles (chaos). Chaotic conditions can be observed by observing the motion of particles that change suddenly, dramatically and tend to

fluctuate, which is indicated by the appearance of whirlpool symptoms with an unpredictable frequency of appearance. The situation as above when compared to the process of whirlwind, it can be a representation of learning about the tornado. Whirlwinds usually occur during the transition season where during the daytime the temperature of hot, stuffy air, and black clouds collect, as a result of solar radiation during the day, clouds form vertically (convective) whose center is low pressure, then in the cloud there is an upheaval or unstable air flow rising and falling at a fairly high speed. Air currents descending at high speed blow to the earth's surface suddenly and travel randomly (Utomo, 2016).

Figure 10 shows that the flow patterns of water particles can be classified into two, namely laminar and turbulent flow. Broadly speaking, the flow of fluid particles is divided into two, namely laminar and turbulent (Jiji, 2006). Between the laminar and turbulent flow patterns, there is a transition state characterized by the speed of the flow of water particles getting faster, the direction of the flow of the particles starting to become irregular and sometimes signs of a water vortex appear. Other information obtained from Figure 9 is that at different thicknesses, the phase transition between laminar and turbulent flows is also different. This difference can be noticed for the water thickness 6 cm experiencing a transition phase faster than the water thickness of 5 cm. Therefore, a water thickness of 6 cm will experience a turbulence phase faster than a thickness of 5 cm. As stated by (Hui Peng, et. al., 2006; Gayen, et. al., 2014 and (Berdnikov, et. al., 2018), the R values for the transition between laminar and turbulent ranged from R=10^6 and R=10^7. By using Table 1 and the approach to the value of the physical properties of water at a temperature of 40°C, the value of R~10^7 at ΔT~ 0°C is obtained for a water thickness of 5 cm, while for a water thickness of 6 cm at ΔT~20°C. If you pay attention to Figure 9, it will show that the observations are in accordance with the theory.

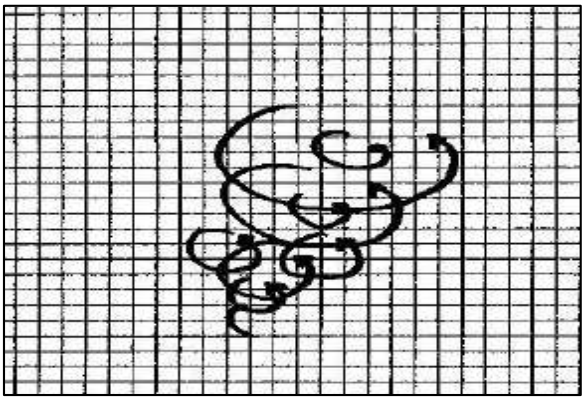

Figure 11. Manual visualization of the whirlpool phenomenon

Figure 11 illustrates the visualization of the whirlpool phenomenon that appears in the transition and turbulent phases (Figure 10). In Figure 11, it can be seen that the whirlpool phenomenon has characteristics, the direction of the flow of the particles is horizontal, the size of the whirlpool is enlarging upward, and the rotation is counterclockwise or turning left (Figure 11). The frequency with which they occur is unpredictable, suddenly and in a short time. This whirlpool appears due to differences in water pressure due to differences in temperature between the bottom and top water particles. Prior to the emergence of the whirlpool, it was observed that SGKJ, as a representation of water particles, moved very rapidly up and down and randomly. SGKJ goes up against the down. The higher the temperature difference, the more frequent whirlpools appear.

As for what happens to the whirlwind phenomenon, namely in the clouds there is an upheaval or unstable air currents up and down at a fairly high speed. Air currents that fall at high speed blow to the earth's surface suddenly and travel randomly (Utomo, 2016). By comparing the two events above, what happens in water fluid can be used to explain the phenomena that occur in wind fluid, for example the emergence of the phenomenon of whirlwind. Whereas regarding the events of the whirlpool spinning counterclockwise or turning left, this is also in accordance with the Buys Ballot Law that the tornado motion in the northern hemisphere is counterclockwise, and the cyclone movement in the southern hemisphere is in the direction of rotation clockwise (Dyahwathi, et. al., 2007). As the limitation regarding fluid above and the ratio between whirlpools and whirlwinds, water fluid is considered a representation of air/wind fluid. In other words, the whirlpool phenomenon can be used as a learning representation of the occurrence of whirlwind natural phenomena.

Conclusion

Based on the results of the research and discussion, it can be concluded that the observation of the convection phenomenon using the RBC observation device can be used as a learning representation of the occurrence of natural phenomena, for example, tornadoes. It was observed that an increase in the temperature difference (ΔT) between the two plates resulted in an increase in the velocity of the motion of the water particles in convection which was depicted by a branching diagram. Due to the difference in temperature (ΔT) also results in the movement patterns of water molecules, namely laminar and turbulent. The turbulent phase with the Rayleigh number value R~10^7, indicated that the flow of water particles is getting faster, the direction of the flow of the particles starts to become irregular and sometimes signs of a water vortex appear. At different fluid immersion results in the start of a turbulent phase. The turbulent phase for d = 5 cm is observed at ΔT~30°C, and d = 6 cm at ΔT~20°C. Furthermore, this RBC phenomenon is

used as a representation of learning natural phenomena in air fluids, namely whirlwinds as an event due to differences in temperature and pressure of a fluid. The use of the observation device should be prepared with a temperature sensor and a high-resolution cam recorder, so that the phenomenon can be clearly observed. Other information obtained from the research is that the temperature difference between the two plates results in an increase in the velocity of the water particles and forms a bifurcation diagram. The flow patterns of water particles were also found due to the temperature difference between the two plates, namely laminar and turbulent, as well as the transition phase between the two.

Acknowledgements

The authors gratefully acknowledge all participants. This study does not use any funding from any institution and no conflict of interests.

References

Ahlers, G., Bodenschatz, E. & He, X. (2017). Ultimate state transition of turbulent Rayleigh Benard convection. *Physical Review Fluids*, *2*(054603), 1–6. https://doi.org/10.1103/PhysRevFluids.2.054603

Ahlers, G. (2006). Experiments with Rayleigh-Benard convection. In book: dynamics of spatio- temporal cellular structures. *Springer Tracts in Modern Physics*, *207*, 67–94. Retrieved from https://link.springer.com/book/10.1007/b106790

Aurnou, J.M. & Olson, P. L. (2001). Experiments on Rayleigh Benard convection, magnetoconvection and rotating magnetoconvection in liquid gallium. *Journal of Fluid Mechanics*, *430*, 283–307. https://doi.org/10.1017/S0022112000002950

Ayed, S.K., Ilic, G., Zivkovic, P., Vukic, M. & Tomic, M. A. (2016). Instability of The Rayleigh-Benard Convection for Inclined Lower Wall with Temperature Variation. *Mechanical Engineering*, *14*(2), 179–197. http://dx.doi.org/10.22190/FUME1602179A

Ayed, S.K., Zivkovic, P. & Tomic, M. A. (2017). Experimental and analytical solution for Rayleigh-Bernard convection. *International Journal of Computation and Applied Sciences*, *3*(2), 224–232.

Ayed, S.K. & Tomic, M. A. (2017). Experiment study of Rayleigh-Bernard convection with upper heat plate effects. *International Journal of Computation and Applied Sciences*, *3*(3), 261–270.

Balasubramanian, S. & Ecke, R. E. (2013). Experimental study of Rayleigh-Bénard convection in the presence of rotation. *International Journal of Materials, Mechanics and Manufacturing*, *1*(2), 148–152. http://dx.doi.org/10.7763/IJMMM.2013.V1.32

Berdnikov, V. S., Vinokurov, V. A., Vinokurov, V. V, Grishkov, V. A., & Mitin, K. A. (2018). Laminar-turbulent transitions at natural convection in flat and annular vertical fluid layers. *Journal of Physics: Conference Series*, *1105*, 12009. https://doi.org/10.1088/1742-6596/1105/1/012009

Bhattacharjee, J. K. (2015). Self-Consistent Field Theory for the Convective Turbulence in a Rayleigh-Benard System in the Infinite Prandtl Number Limit. *Journal Stat Physic*, *2015*(160), 1519–1528. https://doi.org/10.1007/s10955-015-1292-z

Chen, L., Zhao, Y. & Zhang, X. R. (2015). Poiseuille Rayleigh-Benard Convective Flow and Compressible Boundary Effects of Near-Critical Fluid in Microchannels. *Journal of Nanoscienceand Nanotechnology*, *15*(4), 3035–3042. http://dx.doi.org/10.1166/jnn.2015.9653

Drazin, P. G. (2002). *Introduction to hidrodynamic stability*. Chambridge University Press.

Dyahwathi, N., Effendy, S., & Adiningsih, E. S. (2007). Karakteristik badai tropis dan dampaknya terhadap anomali hujan di Indonesia. *Jurnal Agromet Indonesia*, *21*(2), 61–72. https://doi.org/10.29244/j.agromet.21.2.61-72

Fan, X., Wang, S. dan Xu, W. Q. (2020). Initial-Boundary Layer Associated with the 3-D Boussinesq System for Rayleigh-B´Enard Convection. *Electronic Journal of Differential Equations*, *2020*(31), 1–20. Retrieved from https://digital.library.txstate.edu/handle/10877/14535

Gayen, B., Griffiths, R. W., & Hughes, G. O. (2014). Stability transitions and turbulence in horizontal convection. *Journal of Fluid Mechanics*, *751*, 698–724. https://doi.org/10.1017/jfm.2014.302

Getling, A. V. (1997). *Rayleigh Benard Convection; Structures and Dynamics*. Word Scientific.

Green, G., Vlaykov, D.G., Mellado, J.P. and Michael, M. (2020). Resolved energy budget of superstructures in Rayleigh–Bénard convection. *Journal Fluid Mech*, *887*(A21), 1–28.

Grigoriev, V.V. & Zakharov, P. E. (2017). Numerical Simulation of Two-Dimensional Rayleigh-Benard Convection. *AIP Conference Proceedings*, *1907*(030031), 1–8. https://doi.org/10.1017/jfm.2019.1008

Handoko. (1995). *Klimatologi Dasar, Landasan Pemahaman Fisika Atmosfer Dan Unsur Unsur Iklim*. Pustaka jaya.

Hui Peng, S., Davidson, L., & Hanjali, K. (2006). Large Eddy simulation and deduced scaling analysis of Rayleigh Benard convection up to Ra=109. *Journal of Turbulence*, *7*(66), 1–29.

https://doi.org/10.1080/14685240600953462

Jiji, L. M. (2006). *Heat Convection*. Springer-Verlag Berlin Heidelberg.

Klein, M., Schmidt, H. & Lignell, D. O. (2018). Map-based modeling of high-Rayleigh-number turbulent convection in planar and spherical confinements. *Conference on Modelling Fluid Flow (CMFF'18), The 17th International Conference on Fluid Flow Technologies. Budapest, Hungary, September 4-7*, *ISBN 978-9*, 1–8.

Klein, M. & Schmidt, H. (2019). Investigating Rayleigh Benard convection at low Prandtl numbers using one-dimensional turbulence modeling. 11th. *International Symposium on Turbulence and Shear Flow Phenomena, Southampton, UK, July 30 to August 2*, 1–6.

Lyubimova, T.P., Lyubimov, D.V. & Parshakova, Y. N. (2015). Implications of the Marangoni effect on the onset of Rayleigh–Benard convection in a two-layer system with a deformable interface. *European Physical Journal Special Topics*, *224*, 249–259. https://doi.org/10.1140/epjst/e2015-02357-3

Marselina, D.S. & Widodo, E. (2015). Analisis statistika terhadap penyebab angin kencang dan puting beliung di Daerah Istimewa Yogyakarta Tahun 2011-2014. *Jurnal Dialog Penanggulangan Bencana*, *6*(2), 65–80.

Nataraj, S., Reddy K.S. & Thampi, S. P. (2017). Lattice Boltzmann simulations of a radiatively participating fluid in Rayleigh–Benard convection. *Numerical Heat Transfer, Part A: Applications*, *72*(4), 313–329. https://doi.org/10.1080/10407782.2017.1376936

Palymskiy, I. (2015). On Ultimate Regime of Rayleigh-Benard Convection. *Computational Thermal Sciences*, *7*(4), 339–344. http://dx.doi.org/10.1615/ComputThermalScien.2015013665

Pandey, A., Scheel, J.D. & Schumacher, J. (2018). Turbulent superstructures in Rayleigh-Bénard convection. *Article Nature Communications*, *9*(2018), 1–11. https://doi.org/10.1038/s41467-018-04478-0

Ramos, I. C. dan Briozzo, C. B. (2015). Adapting a Fourier pseudospectral method to Dirichlet boundary conditions for Rayleigh–B´enard convection. *Papers in Physics*, *7*, 1–9. https://doi.org/10.4279/pip.070015

Rohman, M. H. (2019). Fenomena Pusaran Air Pada Kajian Konveksi Rayleigh Benard Sebagai Representasi Pembelajaran Terjadinya Angin Puting Beliung. *Jurnal IPA Dan Pembelajaran IPA (JIPI)*, *3*(2), 62–74. https://doi.org/10.24815/jipi.v3i2.14707

Siddheshwar, P. G. and Sri Krishna, C. V. (2001). Rayleigh-Benard Convection In A Viscoelastic Fluid-Filled High-Porosity Medium With Nonuniform Basic Temperature Gradient. *IJMMS*, *25*(9), 609–619. http://dx.doi.org/10.1155/S0161171201001028

Sudia, B. (2017). Konveksi paksa aliran Laminer isotermal di atas plat datar pada berbagai kondisi profil kecepatan. *Dinamika: Jurnal Ilmiah Teknik Mesin*, *9*(1), 6–11. http://dx.doi.org/10.33772/djitm.v9i1.3213

Suparso, E., Rohman, M.H. dan Yusuf, Y. (2010). Kajian Konveksi Rayleigh Benard melalui Pengamatan Gerak Air sebagai Fungsi Ketebalan Air dan Perbedaan Suhu. *Jurnal Fisika Indonesia*, *XIV*(41), 18–28.

Utomo, D. H. (2016). *Meteorologi Klimatologi*. Magnum Pustaka Utama.

Valencia, L. Jordi Pallares, J., Cuesta, I. & Francesc Xavier Grau, F. X. (2007). Turbulent Rayleigh–Be´nard convection of water in cubical cavities: A numerical and experimental study. *International Journal of Heat and Mass Transfer*, *50*(2007), 3203–3215. Retrieved from https://www.sciencedirect.com/science/article/pii/S0017931007000804

Welty, J.R., Wicks, C.E., Wilson, R.E., & Rorrer, G. (2001). *Fundamentals of Momentum, Heat, and Mass Transfer* (4thEd ed.). John Wiley & Sons Inc.

Yustin, R. & Yusuf, Y. (2013). Pengamatan Gerak Konveksi Rayleigh-Benard pada Lapisan Minyak Goreng sebagai Fungsi Ketebalan Lapisan. *Prosiding Pertemuan Ilmiah XXVII HFI Jateng & DIY*, *ISSN: 0853*, 35–39.

Zhou, Z., Liu, K., Xu, L., Zhang, G., Wang, Z., Ren, T., Gu, C. & Sun, G. (2019). Study on propagation characteristics of laser in turbulent Rayleigh–Bénard thermal convection. *Journal of Engineering*, *2019*(20), 6902–6905